Available at www.sciencedirect.com

ScienceDirect

journal homepage: www.elsevier.com/locate/he

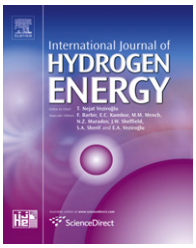

High growth rate, photosynthesis rate and increased hydrogen(ases) in manganese deprived cells of a newly isolated *Nostoc*-like cyanobacterium (SAG 2306)

R. Abdel-Basset [a,*], *T. Friedl* [b,1], *K.I. Mohr* [b,1,2], *N. Rybalka* [c,3], *W. Martin* [d,4]

[a] *Botany department, Faculty of Science, Assiut University, 71516 Assiut, Egypt*
[b] *Experimental Phycology and Culture Collection of Algae, Georg-August University Göttingen, Untere Karspüle 2, 37073 Göttingen, Germany*
[c] *Plant Cell Physiology and Biotechnology, Botanical Institute and Botanical Garden, Christian Albrechts University Kiel, Am Botanischen Garten 1-9, 24118 Kiel, Germany*
[d] *Institut für Botanik III, Heinrich-Heine Universitaet Düsseldorf, Universitätsstr. 1 40225 Düsseldorf, Germany*

ARTICLE INFO

Article history:
Received 16 February 2011
Received in revised form
29 June 2011
Accepted 3 July 2011
Available online 5 August 2011

Keywords:
Manganese deprivation
Photosynthesis
Respiration
Hydrogenases
Nostoc

ABSTRACT

A *Nostoc*-like cyanobacterium, strain SAG 2306, was isolated from a clay soil sample at Assiut region (Egypt). Morphology and analysis of 16S rDNA identified it as a member of the heterocyteous cyanobacteria (Nostocales). Unexpectedly, chlorophyll *a* and dry weight were higher in manganese deprived (Mn-) or in manganese double deprived (Mn–) than in replete (Mn+) cells. The latter phase of Mn– diluted the cellular content in daughter cells to a critical minimal value of about 1.5% relative to the original 100% in Mn+. Similar to growth, *Nostoc* sp. exhibited a significant age-dependent biphasic impact on hydrogenases activity. Older cells of 120 h age displayed higher hydrogen evolution rates than younger ones. The results suggest inhibitory effects of the 12 μM manganese contained in BG11 medium (Mn+) not only on growth but also on hydrogen production during the first 72 h of growth.

1. Introduction

Two main prerequisites are needed for biological hydrogen production: electron sources and active enzymes. The electron supply in bacteria (performing non-oxygenic photosynthesis) would be derived from oxidation of organic matter. Organic wastes being intensively tested include different types of agricultural, industrial, domestic wastewater and sewage [1,2,3,4]. In cyanobacteria (oxygenic photosynthesis), water is the electron source for hydrogen evolution. The enzymes - hydrogenases and nitrogenases - are, however, oxygen labile. Therefore, oxygen and hydrogen evolution must be separated or oxygen evolution must be hindered to allow hydrogen production. One approach is to lower photosynthetically

* *Corresponding author*. Tel.: +20 88 241 2297; fax: +20 88 234 2708.
E-mail addresses: rbasset@aun.edu.eg (R. Abdel-Basset), tfriedl@uni-goettingen.de (T. Friedl), kathrin.mohr@helmholtz-hzi.de (K.I. Mohr), nrybalk@uni-goettingen.de (N. Rybalka), w.martin@uni-duesseldorf.de (W. Martin).
[1] Tel.: +49 551 397868; fax: +49 551 397871, http://www.epsag.uni-goettingen.de.
[2] present address: Helmholtz Centre for Infection Research, Research Group Microbial Drugs, Inhoffenstrasse 7, 38124 Braunschweig, Germany.
[3] Tel.: +49 551 3915068; fax: +49 551 397871, http://www.uni-kiel.de/Botanik/RSchulz/index.html.
[4] Tel.: +49 211 811 3011; fax: +49 211 811 3554, web: http://www.molevol.de.
0360-3199/$ – see front matter
doi:10.1016/j.ijhydene.2011.07.006

evolved oxygen as much as possible. This might be achieved via manganese limitation since Mn plays a central role in PSII-catalyzed water oxidation, electron transfer and oxygen evolution. The photosynthetic water oxidizing complex contains a manganese cluster of four atoms, donating electrons to redox-active tyrosine (Yz) on D1 protein. The Kok model [5,6] explains the pattern of oxygen evolution by introducing five discrete oxidation states (S-states), S_0, S_1, S_2, S_3, and S_4 of the manganese cluster. The role of Mn in PSII-catalyzed water oxidation has been reviewed [7,8]. Recently, it has been indicated that the fast electrogenic component in PSII could be ascribed to reduction of Y_Z^{ox} by Mn [9].

In addition to water oxidation, Mn is involved in several other redox reactions and antioxidant enzymes, prominent among which is manganese superoxide dismutase (MnSOD). In the cyanobacterium *Nostoc* sp. PCC 7120, a membrane-associated MnSOD protects the photosynthetic apparatus and nitrogenase from oxidative damage [10]. SOD is a critical component of the ROS (reactive oxygen species) scavenging system in plant chloroplasts [11]. Manganese deficiency in *Chlamydomonas* results in loss of photosystem II and MnSOD function and subsequent sensitivity to peroxides [12]. Thus, the prime targets of Mn deficiency in plants are PSII and MnSODs [13]. In addition, secondary iron and phosphorus deficiency, along with their consequent drawbacks, result from Mn deficiency [12].

Strikingly, hydrogenases have been found to exert a protective role in cells exposed to manganese deficiency. Early reports indicated that algae without hydrogenase become rapidly chlorotic under manganese deficiency while chlorophyll is much more stable in those containing hydrogenase [14]. Also, the cyanobacterium *Synechococcus elongatus* PCC 7942 (previously known as *Anacystis nidulans*) develop chlorosis, like higher plants, under manganese deficiency because it does not have hydrogenase [15]. Since hydrogenase is inactive under aerobic conditions, it is conceivable that *S. elongatus* PCC 7942 might make internal use of hydrogen donors other than molecular hydrogen [14]. In this work, depleting manganese from cells of the *Nostoc*-like strain SAG 2306 has been anticipated to limit oxygen evolution, enhance anaerobiosis and upregulating hydrogenases activity, preferably with minimal drawbacks on growth.

2. Materials and Methods

A cyanobacterial strain has been isolated from a clay soil sample at Assiut region (Egypt) and tentatively identified as *Nostoc* sp. as it forms unbranched filaments with heterocytes. The isolate has been accessioned by the Culture Collection of algae at Göttingen University, Germany (SAG; www.wpsag.uni-goettingen.de) as strain SAG 2306 after purification into axenic culture.

2.1. Morphological examination

The morphological examination of strain SAG 2306 was performed on cultures grown in liquid standard BG-11 medium [16] maintained at 18 °C under a light/dark regime of 14 h:10 h and a photon fluence rate of about 20 μmol photons m^{-2} s^{-1} from white fluorescent bulbs. The studied cultures were 5 and 12 months old. Highest heterocyst formation was observed in nitrogen deprived medium [17]. Heterocysts were photographed using a Leica microscope (DM LB2) equipped with a DFC280 Leica Camera (equipment donation from AvH to Prof. Dr. M. S. Mahmould, Assiut University, Egypt).

2.2. Molecular characterization

To confirm its identification and to determine its phylogenetic position, 16S rDNA sequence comparisons were performed. DNA extracted from a liquid culture of strain SAG 2306 after cell breakage using glass beads in a MinibeadbeaterTM cell homogenizer (Biospec, Bartlesville, USA) with the Invisorb Spin Plant Mini Kit (Invitrogen, Karlsruhe, Germany) according to protocols provided by the manufacturer. The 16S rRNA gene sequence was amplified using primer pair PCR1 and PCR 18 [18]. PCR amplification conditions and cycle-sequencing were as described [19]. The 16S rDNA sequence from strain SAG 2306 was subjected to the BLASTn search tool (www.ncbi.nlm.nih.gov/BLAST/) in order to retrieve the closest relative sequences. Because the results confirmed SAG 2306 to be a member of heterocyteous cyanobacteria (Nostocales [20], or Subsection IV [21], the sequence was compared with other sequences representing heterocyteous cyanobacteria using the large 16S rDNA sequence database maintained in the ARB program (version 05.05.26 [22]. This database was updated with all 16S rDNA sequences available for the heterocyteous cyanobacteria. A subset of these sequences comprising a total of 62 complete 16S rDNA gene sequences (1438 bp long; 370 variable/292 informative sites) for representatives of heterocyteous cyanobacteria and three sequences of *Chroococcoidopsis* (AB039005, AJ344552, AJ34553) to root the phylogeny (based on the finding that this genus forms the next closest relatives to heterocyteous cyanobacteria [23] were extracted from the ARB database and subjected to Maximum Likelihood analyses using the program Treefinder [24]. The optimal model of sequence substitution was selected using the AIC criterion in Treefinder. The GTR model [25] was selected with the rate parameters set to optimal and frequency parameter estimated empirically assuming a discrete Gamma model for the heterogeneity of rate of substitutions with the number of rate categories = 5. Confidence values for the obtained groups (edge support) were inferred from expected-likelihood weights [26] applied to local rearrangements (1000x, search depth = 2) of the tree topology as provided in Treefinder. Only values at or over 87% were recorded. Pairwise sequence difference (total sequence differences and Kimura 2-parameter corrected distances) were calculated in MEGA 3.1 [27]. The phylogeny is presented in Fig. 2. The clades I - IV correspond to clades of heterocyteous cyanobacteria as presented previously [28]. Clades of true-branching heterocyteous cyanobacteria are indicated by numbers 1 -3 and 5 following ref. [29,30]. In Fig. 2, for clarity, some groups of sequences were collapsed into triangles. They correspond to the following clades of the phylogeny and include the following sequences: clade I, *Nostoc edaphicum* AJ630449, *N. microscopicum* GQ287653, *N. punctiforme* GQ287652, *N.* sp. AM711522, AY742451, AY742453, DQ185252, AF027655, and AJ344563; clade IV, *Anabaena augstumalis* AJ630458, *A. circinalis*

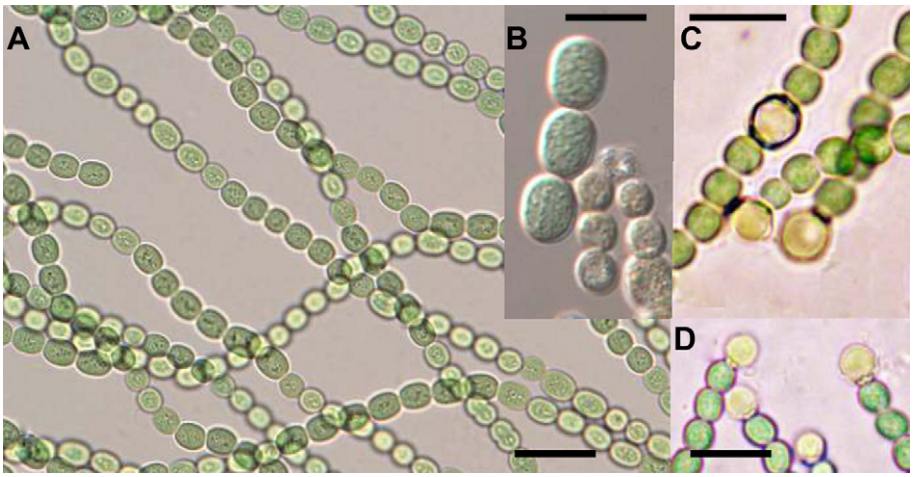

Fig. 1 – Morphology of strain SAG 2306. (A) Filaments of a young culture. (B) Akinetes in a short chain, old culture. (C, D) Terminal and intercalary heterocytes. Scales, 10 μm.

AJ133156, *A. compacta* AJ630418, *A. oscillarioides* AJ630426, AJ630428, *Aphanizomenon flos-aquae* AJ630442, *Coleodesmium* sp. AY493596, *Cylindrospermopsis raciborskii* AF092504, *Nodularia harveyana* AM711554, *N.*sp. AM711553, *Nostoc elgonense* AM711548, *Ns.* sp. AM711525, *Tolypothrix distorta* GQ287651, *Trichormus variabilis* AJ630456; clade 1, *Fischerella muscicola* AJ544077, *F.* sp. AJ544076, *Hapalosiphon welwitschii* AY034793, *Nostochopsis lobatus* AJ544080, *Npsis.* sp. AJ544081, *Westiellopsis prolifica* AJ544086, and AJ544087; clade *Scytonema*, *S. hofmanni* AB075996, AF132781, and *S.* sp. AY069954.

For physiological studies, SAG 2306 was grown under a light intensity of 110 μmole photons m^{-2} sec^{-1}, shaken at 125 rpm (GFL, Burgwedel, Germany) at 30°C ± 0.1. Control cultures were grown in full strength BG11 medium [16] containing 12 μM Mn (Mn^{+}). Manganese-deprived medium was prepared by replacing $MnCl_2$ of BG11 with KCl to remove Mn and maintain Cl contents at the same time. Inoculum aliquots (72 h old cells) were centrifuged; old medium decanted and only cells were then resuspended in the new medium. Chlorophyll *a* content at zero time was determined; its values are not given but included in the calculations of chlorophyll doublings and Mn contents (explained in the next paragraph). Manganese deprivation was conducted by transferring identical amounts of inoculum (of the same age, culture and containing the same amount of chlorophyll *a* as in Mn+) into manganese deprived BG11 (Mn-). In the case of manganese double deprivation (Mn–), however, the inoculum is identical in amount and age but taken from Mn- cells and let grown again in Mn- medium.

Manganese contents of Mn- and Mn– in strain SAG 2306 cells were calculated relative to [Mn^{+}] of BG11. Calculations are based on the rationale that the number of chlorophyll *a* doublings (NCD) by the end of growth period indicates and equals the number of dilutions (ND) of Mn contents into daughter cells that took place during cell division. NCD has been calculated by dividing chlorophyll *a* content of 72 h or 120 h old cells by the chlorophyll *a* contents of the inoculum cells at zero time. Assuming that inoculum cells (Mn+) contain 100 units (or 100%) of manganese, divided by number of dilutions (ND) in Mn- and Mn– gives mathematical estimate of manganese contents.

Growth rate ($\mu \cdot h^{-1}$) was calculated as $[(\ln(A_1) - \ln(A_0)]/(t_1-t_0)$ as in ref. [31]. A_1 and A_0 are the chlorophyll *a* contents at t_1 and t_0 times; respectively. Generation time (G h^{-1}) was calculated as $\ln(2)/\mu \cdot h^{-1}$.

Chlorophyll *a* was extracted in 90% hot methanol, measured and calculated using the equations of ref. [32]. Dry matter was estimated for aliquots of cyanobacterial suspension (50 ml), filtered through filter paper (Whatmann filter paper No. 1) and oven dried for 18 h at 80 °C. Oxygen exchange (photosynthesis and respiration) was measured using the fiber-optic oxygen meter, Microx TX3 (PreSens, Precision sensing GmbH, Regensburg, Germany) repeatedly used for similar purposes [33]. Photosynthesis (P_N) was measured at two light intensities representing the light intensity at which the cyanobacterium was grown (growth light) and the saturating light to explore maximum photosynthetic capacity (saturating light). These were 110 and 2000 μmole photons$\cdot m^{-2}$ s^{-1}; respectively from S light source (cold light lamp Eschenbach, Germany) measured by quantum sensor (Sky Instrument, UK).

Hydrogen evolution was monitored also using a Clark-type oxygen electrode adjusted to hydrogen measurement (instead of oxygen) as instructed by Hansatech Inc. and the protocol used in ref. [34]. Aliquots of *Nostoc* sp containing 1–3 μg Chl a$\cdot ml^{-1}$ (depending on the treatment) were centrifuged, medium decanted and resuspended in 1 ml Mops buffer (50 m M, pH6.8) free from any combined nitrogen. After being transferred to the cell of the oxygen electrode that was tightly covered with a silicon disc through which nitrogen flushing for 15 min took place. Dark and light assays of hydrogen were monitored. After 10 min, the dark H_2 evolving system was illuminated by the high light intensity. Light evolution of hydrogen was steep and lasted for only 15–20 min before it leveled off and declined under light; most probably by the accumulated oxygen.

Uptake hydrogenase was assayed by the reduction of methylene blue essentially according to ref. [35]. Intact

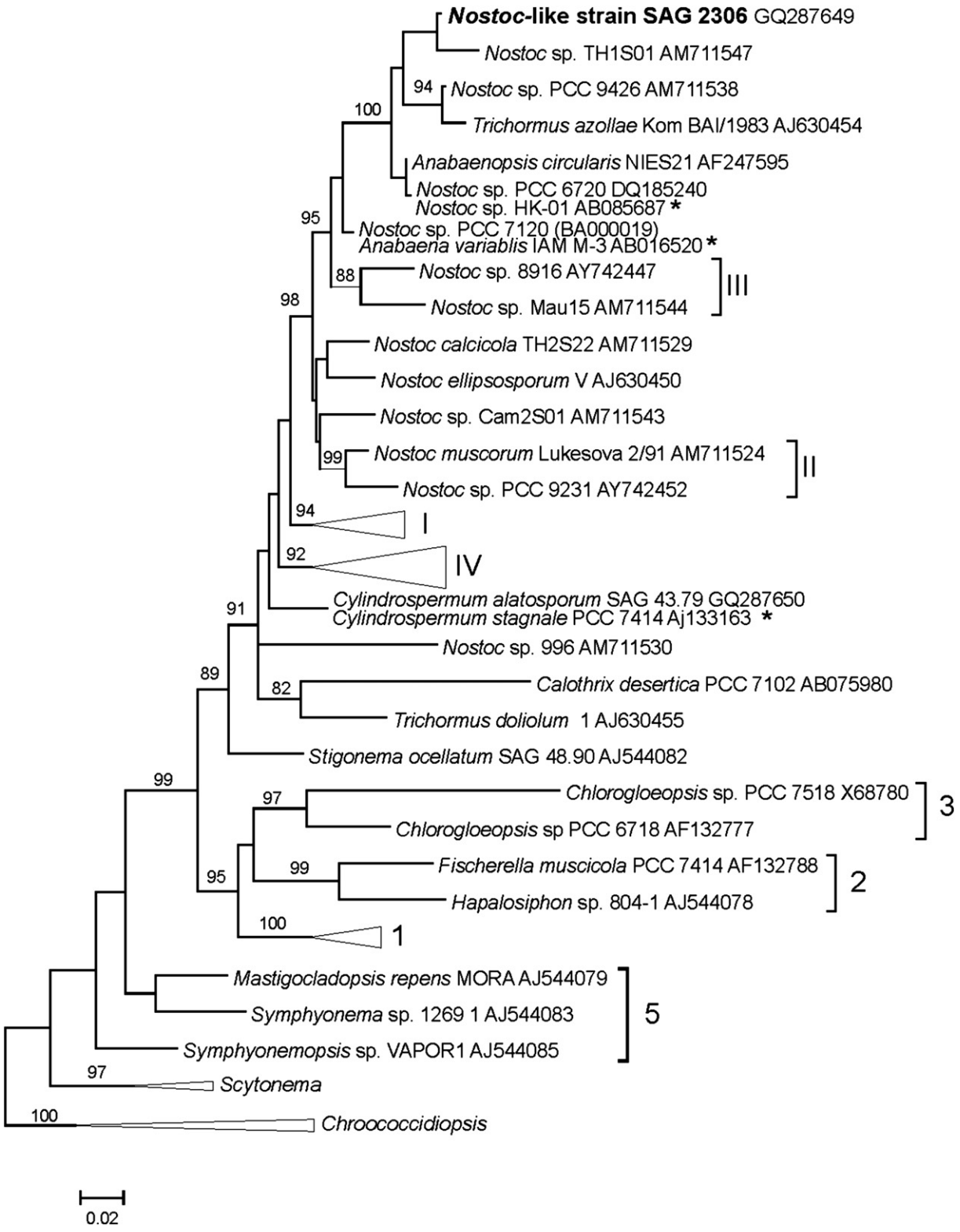

Fig. 2 – Maximum likelihood phylogeny of heterocyteous cyanobacteria demonstrating the phylogenetic position of strain SAG 2306. Sequence accession numbers are given right to species names. Numbers at internal branches correspond to confidence values for the obtained groups. An asterisk indicates cyanobacterial strains which shared almost identical sequences with other sequences from the data set and, therefore, were not used in the phylogenetic analyses, but simply added to the figure. Clades I Iv, 1-3 and 5 correspond to clades of heterocyteous cyanobacteria as presented previously (see Materials and Methods).

cyanobacterial suspensions of 72 h and 120 h old cells containing 3–4 μg chlorophyll *a* (varied according to the Mn treatment) were centrifuged, concentrated to 0.2 ml and used in assay. The reaction assays mixtures were flushed with hydrogen gas for 1 min in specially designed spectrophotometric cells. The decreased absorbance of methylene blue was measured and recorded using spectrometer (R.29: Pharmacia Biotech, Uppsala; now: GE Healthcare Munich; Ultrospec 2000, UV/Visible Spectrophotometer). The evolution activity of the biodirectional hydrogenase was monitored using assay mixtures similar to those used in ref. [36]. The assay depends on dithionite reduced methyl viologen as the electron donor after nitrogen flushing.

Analysis of variance (F values) between manganese levels at each age, between the two ages at each Mn level and their interactions (age × Mn) was calculated using SAS statistical program whereas SPSS program was used to determine the significant difference between means using one way ANOVA test.

3. Results

3.1. *Morphology, identification and phylogenetic position of strain SAG 2306*

The unbranched uniseriate trichomes were almost straight, only slightly waved, and consisted of vegetative cells with the dimensions of 7.3 (5.6) 3.7 μm × 6.7 (5.4) 4.3 μm (length × width: max. (mean) min.; Fig. 1A). Terminal cells of the trichomes were of the same size as the intercalary vegetative cells. No hormogonia were observed and no mucilaginous envelope of trichomes was detected. Heterocytes were formed at terminal ends of the filaments and intercalary, of ovate shape and about the same size as vegetative cells (Fig. 1C,D). Akinete-like cells were of the same shape as vegetative cells, but slightly larger with the dimensions of 9.5 (7.6) 5.6 μm × 7.6 (6.3) 5.2 μm (length × width: max. (mean) min.) with a more granular structure and sometimes connected to short chains which frequently occured in old cultures (Fig. 1B). Analyses of the 16S rDNA sequence from strain SAG 2306 substantiated that it is a member of Nostocales (Subsection IV). BLASTn database searches revealed highest sequence similarities of 97% and 96% with strains assigned to *Nostoc* (strains TH1S01, PCC 6720, PCC 7120 and PCC 9426), *Trichormus azollae* Kom BAI/1983, *Anabaena variablis* IAM M-3 and *Anabaenopsis circularis* NIES 21. In the phylogenetic analyses strain SAG 2306 was nested within a well supported monophyletic clade representing all the aforementioned strains except strains PCC 7120 and IAM M-3 which formed a lineage outside of this clade (Fig. 2). Strain SAG 2306 had the shortest genetic distance (0.019, corresponding to 26 sequence differences) with strain *Nostoc* sp. TH1S01, then the next shortest distances were with *A. circularis* (0.022; 30 sequence differences) and strains *N.* sp. PCC 6720 and HK-01 (0.024; 32 sequence differences).

3.1.1. *Growth*

Growth of *Nostoc* strain SAG 2306 in manganese replete (Mn+) as well as in manganese deprived (Mn-) BG11 nutritive medium was assessed by daily increments in chlorophyll *a* contents. The first noticeable observation in strain SAG 2306 growth was the extended lag phase that lasted for up to 4 days (96 h) before getting into the phase of logarithmic growth which continued for a long period of time (Fig. 3). However, sampling problems due to the formation of filamentous aggregates and the subsequently missed accuracy urged to stop pursuing physiological studies by day 5 (120 h) in all the other next experiments. For this reason, also, optical density measurements become invalid at later and dense stages of growth. The second observation in Fig. 2 is the (unexpected) higher growth rate and magnitude (with relatively shorter lag phase) of the manganese deprived cells (Mn-) than those of manganese supplemented cells (Mn+). Enhanced growth in manganese deprived cells led to further deprive manganese from strain SAG 2306 cells. This was conducted by inoculating manganese deprived cells (Mn-) into fresh manganese-free medium and let them grow 5 days more. Repeated cell division of previously deprived cells will further dilute manganese contents in the daughter cells; in this case these cells will be (and referred to throughout the text as) manganese double deprived (Mn–). Table 1 shows the calculations of manganese contents. Manganese concentrations dropped in the first 72 h to 14 and 1.5% the control value in Mn- and Mn– cells; respectively. Further enhancement of chlorophyll *a* contents was nevertheless as follows: Mn– >Mn-> Mn+ (Fig. 4A). Another approach for diluting cellular manganese contents was extending growth in respective media for two more days i.e. up to 120 h. In this case, manganese calculations revealed low values of only 7.0 and 0.8% that of the control in Mn- and Mn–; respectively (Table 2). Only at this stage (120 h) control cultures grew faster than manganese deprived cultures (Fig. 4A) indicating that manganese limitation become a growth limiting stress. From 72 h to 120 h, chlorophyll *a* was multiplied three times in Mn + while only 1.9 and 1.6 in Mn- and Mn–, respectively. Generation time and growth rate on chlorophyll basis are presented in Table 3. Growth rate was

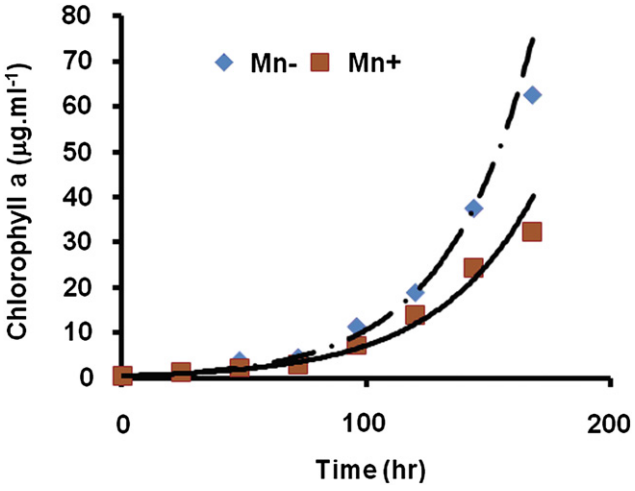

Fig. 3 – Growth curve of the *Nostoc*-like strain SAG 2306 assessed by daily measurement of chlorophyll (a) contents. The strain was grown in manganese replete (Mn+) and manganese deprived (Mn-) BG11 medium.

Table 1 – Mathematical manganese contents of strain SAG 2306 cells supplemented with manganese (Mn+), manganese deprived (Mn-) and manganese double deprived (Mn–). ND is the number of dilutions of cellular manganese which equals the number of chlorophyll doublings (NCD); see "Materials and Methods".

	NCD = ND		Mathematical Mn content (%)	
	72 h (mean ± SE, $n = 15$)	120 h (mean ± SE, $n = 11$)	72 h	120 h
Mn+	4.638 ± 0.97	13.960 ± 2.90	100	100
Mn-	7.329 ± 1.29	14.301 ± 4.14	13.64	6.99
Mn–	9.093 ± 1.10	16.786 ± 2.89	1.50	0.80

enhanced and subsequently the generation time was shortened by manganese deprivation and further by double deprivation in 72 h old cells. However, extending growth for two more days reversed the impact of Mn deprivation, rendering it inhibitory to growth rate and prolonging the generation time to more than twice that in 120 h old cells. Subsequent to such biphasic growth pattern, characterization of photosynthesis, respiration and hydrogenases activity were followed in 72 h old cells (late lag phase) and 120 h old cells (mid log phase).

A similar manganese-related effect was also observed in dry mass accumulation. In 72 h old strain SAG 2306 cells, dry matter accumulation was enhanced by manganese deprivation and even more by double deprivation (Fig. 4B) but differences were relatively less pronounced than those of chlorophyll *a*. Cells, 120 h old, lost their preferential response to manganese limitation and the extent of growth become similar. It can be concluded that manganese content in BG11 medium seems inhibitory to strain SAG 2306 cells in the lag phase of growth (the first 72 h). After being diluted throughout the log phase Mn rendered a stimulatory concentration.

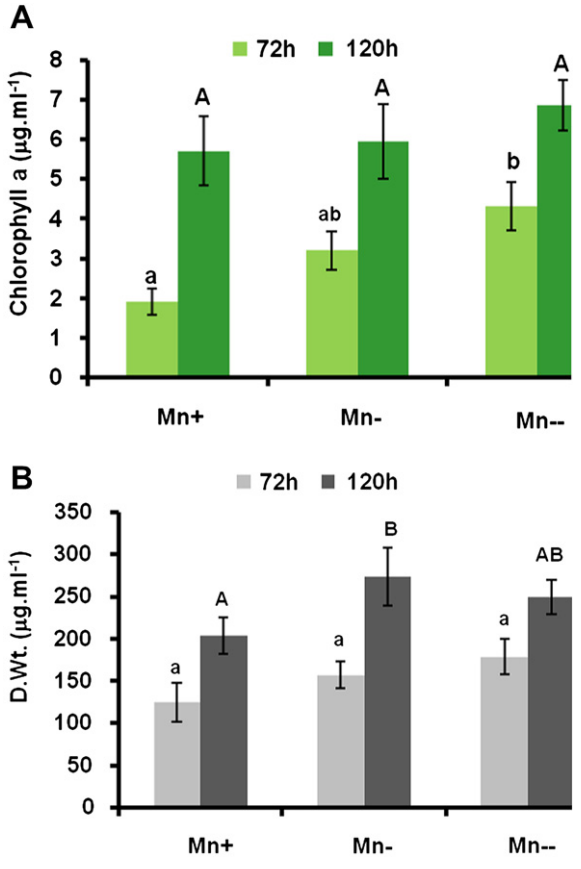

Fig. 4 – (A) Chlorophyll *a* content of *Nostoc*-like strain SAG 2306 grown in manganese replete (Mn+), manganese deprived (Mn-) and manganese double deprived (Mn–) BG11 medium. Presented data are means ± SE ($n = 15$ and 6 for 72 h and 120 h; respectively). Different letters indicates statistical significance between Mn treatments of the same age, small for 72 h and capital for 120 h at the 5% confidence level. (B) Dry matter of *Nostoc*-like strain SAG 2306 grown and statistically presented as in Fig. 3. Presented data are means ± SE ($n = 10$ and 6 for 72 h and 120 h; respectively).

3.2. *Hydrogenases and hydrogen evolution*

Uptake hydrogenase (Hup) activity was enhanced by manganese deprivation in the 72 h old cells (Fig. 5A). The rate was about 50% higher in Mn- than in control cultures (Mn+). Double deprivation (Mn–), however, did not induce further pronounced enhancement. Aging to 120 h enhanced uptake hydrogenase activity only in control cultures while lowered that of Mn deprived (Mn- or Mn–) cells. Evolution activity of Hox (the bidirectional enzyme) was not enhanced in 72 h manganese deprived (Mn-) cells but double deprivation exerted a noticeable stimulation up to 140% that of the control culture (Fig. 5B). Much more enhancement was induced by aging to 120 h, the highest value was in Mn- that surpassed 170% that of the 72 h cultures. Enhanced evolution activity by aging might be attributed primarily to the inhibited uptake (compare Fig. 5A and B). In terms of bioenergetics, enhanced energy loss (H_2 evolution), less energy recovery (inhibited uptake) align with inhibited growth rates in Mn deprived 120 h

Table 2 – Growth rate and generation time of SAG 2306 cells supplemented with manganese (Mn+), manganese deprived (Mn-) and manganese double deprived (Mn–) grown for 72 h and 120 h (means of 15 and 11 replicates, respectively).

	Growth rate ($\mu.h^{-1}$)[a]		Generation time ($G\ h^{-1}$)	
	72 h	120 h	72 h	120 h
Mn+	0.020	0.023	35.2 ± 0.2	30.5 ± 0.2
Mn-	0.026	0.013	27.1 ± 0.1	53.7 ± 0.3
Mn–	0.030	0.010	23.0 ± 0.1	72.0 ± 0.4

a Standard errors in growth rates were about ±0.001.

Table 3 – Analysis of variance (F values) for the effect of manganese (Mn), age and their interaction on the various parameters studied in the cyanobacteium *Nostoc* sp SAG 2306.

SOV/Parameter	Chl.	D. Wt.	H_2D	H_2L	P_NLL	P_NHL	R_D	CP	P/R LL	P/R HL	Hup	Hox
age	44.72 **	32.48 **	210.62 **	186.71 **	12.86 **	9.18 **	9.98 **	14.04 **	8.91 **	0.85 ns	2.97 **	38.50 **
Mn	5.16 **	4.71 *	2.72 ns	10.31 **	0.64 ns	0.25 ns	1.87 ns	1.57 ns	2.25 ns	2.14 ns	0.20 ns	2.68 ns
Age × Mn	0.74 ns	0.83 ns	0.36 ns	14.78 **	1.34 ns	0.59 ns	1.77 ns	0.59 ns	0.73 ns	0.37 ns	3.16 ns	1.13 ns

Chl. (chlorophyll) a, D. Wt. (dry weight), H_2D & H_2L (hydrogen gas evolution in the dark and light; respectively), P_NLL and P_NHL (net photosynthesis at low and high light intensity; respectively), R_D (Dark respiration), CP (compensation point), P/RLL and P/RHL (photosynthesis/respiration ratio at low and high light intensity; respectively, Hup and Hox are uptake and bidirectional hydrogenases activity; respectively, SOV (source of variance), ns (not significant),*, ** (significant and highly significant; respectively).

old cells. It is questionable whether slowed growth rate (less energy demands) saved H_2 for evolution or less energy recovery from oxidation activity by Hup slowed growth.

Hydrogen evolution was detected in all cultures of *Nostoc* sp exposed to various treatments of manganese (Fig. 5C). Highest rates of nearly 143, 252 and 350 μmole $H_2 \cdot mg^{-1}$ Chl$\cdot min^{-1}$ in Mn+, Mn- and Mn–; respectively were evolved in 120 h old cells of *Nostoc* cells under high light conditions. However, traces of hydrogen ranging from 1 to < 14 μmole $H_2 \cdot mg^{-1}$ Chl$\cdot min^{-1}$ were recorded in other cultures (dark of 72 h, 120 h and dark of 120 h old). In all cases, light-dependent hydrogen evolution continued for a period of 10–20 min before declining.

3.3. *Photosynthesis and respiration*

Chasing the point at which oxygen evolution and accumulation exhibited its minimal levels (hydrogenases activity prerequisite) necessitates characterizing photosynthesis in strain SAG 2306. The photosynthetic oxygen evolution (P_N) was estimated under two light intensities; low of 110 and high of 2000 μmole photons.m^{-2}.sec^{-1} which represent growth and saturating light, respectively. Unlike its stimulant effect on biomass (chlorophyll or dry matter) manganese deprivation inhibited photosynthesis. At low light (LL), P_N of Mn- dropped to 70% relative to that of the control culture (Mn+). However, manganese double deprivation (M–) induced comparatively only marginal further decrease in the rate of oxygen evolution (Fig. 6A); a value of less than 10% relative to that of Mn-. Conspicuous inhibition of photosynthesis was observed by aging to 120 h. P_N of control cultures dropped from 0.81 at 72 h to 0.27 μmole $O_2 \cdot mg^{-1}$Chl$\cdot min^{-1}$ at 120 h (65% inhibition). A similar inhibition but less in magnitude, was observed in manganese deprived cells (Mn-); inhibition was about 50%. The least but also obvious inhibition related to aging was recorded in M– (only 30%). Inhibition by aging was higher than by manganese deprivation but it is noteworthy to remind that aging or time *per se* implies manganese dilution into daughter cells during repeated division. High light intensity (HL) remarkably enhanced oxygen evolution (Fig. 6B). The control rate elevated from 0.8 to 1.8 μmole $O_2 \cdot mg^{-1}$Chl$\cdot min^{-1}$ at low *vs.* high irradiance. The ratio of light intensities was about 18 times (HL/LL) while photosynthetic rate was enhanced by a factor of only 2.25 times (HL/LL). The inhibitory effect of manganese deprivation (Mn- or Mn–) on P_N was much less pronounced at HL compared with that at LL. Similar with that at LL, strain SAG 2306 cells of 120 h old exhibited lower rates of photosynthesis relative to 72 h old cells to both light intensities. No preferential inhibitory effect of manganese deprivation would be inferred at this age; otherwise a slight increase can be seen at both light intensities.

Compensation point at high light intensity was about 200 μmole $O_2.mg^{-1}$Chl.min^{-1} in control cultures (Mn+) of strain SAG 2306 (Fig. 6C). Manganese deprivation (Mn-) severely lowered compensation point to one quarter the control value (i.e. 50 μmole $O_2 \cdot mg^{-1}$Chl$\cdot min^{-1}$) but no further decrease imposed by double deprivation (Mn–). Aging to 120 h sharply dropped the compensation point in control cultures but markedly less in manganese deprived or double deprived; rendered all values of compensation point similar regardless of manganese status.

Respiratory oxygen uptake of 72 h old cells was slightly lowered by manganese deprivation but more remarkably by double deprivation (Fig. 6D). Aging until 120 h inhibited respiration of control and manganese deprived cultures but very slightly in double deprived; leading to the observation that all cultures displayed similar respiration rates despite variation in Mn availability.

The above-described experimental data were subjected to statistical analysis twice. The two-way ANOVA (Table 3) shows that the effect of manganese as a single factor was significant only on chlorophyll, dry mass and the light-induced evolution of hydrogen. The effect of age, however, was highly significant on all of the studied parameters (chlorophyll *a*, dry mass, dark and light evolution of hydrogen, photosynthetic evolution, respiration, compensation point and hydrogenases activity of both uptake and bidirectional enzymes). Interactive effects (age × Mn) exhibited its significance exclusively in the case of the light-induced hydrogen evolution (Table 3). Further analysis of the data indicated that manganese double deprivation was the most effective treatment. This effect is shown on graphs as small and capital letters for 72 h and 120 h; respectively.

4. Discussion

The sequence comparisons revealed strain *Nostoc* SAG 2306 as a very close relative to strain *Nostoc* sp. THS01 which was isolated from a rice field in Thailand [28], but the strain was together with members of *Anabaenopsis* and *Trichormus* in the same clade which was well supported in the phylogenetic analyses (100% internal edge support; Fig. 2). This clade is clearly separated from strain PCC 7120 which is often regarded

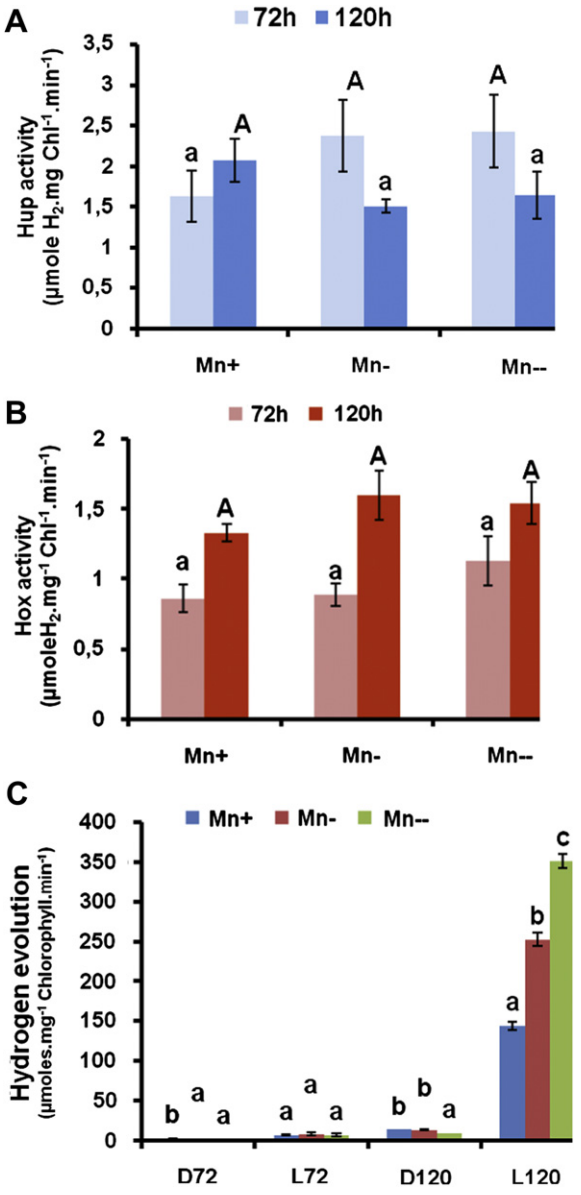

Fig. 5 – (A) Uptake hydrogenase activity of (Mn+, Mn- and Mn–) *Nostoc*-like strain SAG 2306 assayed in the dark. Presented data are means ± SE (n = 10 and 6 for 72 h and 120 h; respectively). Statistical presentations are as in Fig. 3. (B) Evolution activity of the bidirectional hydrogenase of (Mn+, Mn- and Mn–) *Nostoc*-like strain SAG 2306 assayed in the dark. Presented data are means ± SE (n = 3 and 3 for 72 h and 120 h; respectively). Statistical presentations are as in Fig. 3. (C) Hydrogen gas evolution by (Mn+, Mn- and Mn–) *Nostoc*-like strain SAG 2306. D means dark, L means light; 72 h and 120 h refer to cell ages. Presented data are means of at least three replicates. Statistical presentations are as in Fig. 3.

as an important reference strain to represent the genus *Nostoc*. Thus, no unambiguous assignment at the generic level was possible. The clade with strain SAG 2306 is another deeply diverging clade on which strains assigned to *Nostoc* are distributed in the 16S rDNA phylogenetic analyses, in addition to the clades I - IV previously resolved [28]. The heterocyteous cyanobacteria are in urgent need of taxonomic revision and a future study must clarify which of the several lineages and clades represents the "true" genus *Nostoc* while each of the other clades represents another genus of Nostocales. Furthermore, our phylogenetic analyses are in agreement with previous findings regarding the phylogeny of heterocyteous cyanobacteria. The Nostocales [20] or Subsection IV cyanobacteria [21] which include non-branched and false-branching (*Scytonema*) heterocyteous strains form a monophyletic lineage (91% internal edge support; Fig. 2). The lineages of the true-branching heterocyteous taxa (former order Stigonematales [25],; Subsection V [21]. are, in concordance with ref. [22], distributed on several lineages (1, 2, 3, *Mastigocladopsis/Symphyonema*, and *Symphyonemopsis*; Fig. 2).

The *Nostoc*-like strain SAG 2306 grew very efficiently, with relatively long lag phase (96 h), on 12 µM manganese originally contained in BG11 nutritive medium (Mn+). Mn deprivation noticeably enhanced chlorophyll and dry matter increments in cells of the strain. Growth rate was enhanced and subsequently the generation time was shortened by manganese deprivation (Mn-) and further by double deprivation (Mn–) throughout the first 72 h of growth. In other words, the concentration of 12 µM Mn in Mn replete medium (Mn+) slowed down chlorophyll increments and seems high enough to be inhibitory. Extending growth, however, for two more days reversed this impact i.e. Mn deprivation became inhibitory to growth rate and thus the generation time prolonged to more than its double in the last 120 h. Growth in manganese deprived media, *per se*, implies further deprivation by diluting Mn contents of the inoculums cells into daughter ones during repeated cell division. A critical minimal content of cellular manganese (mathematical) is attained and become retarding in Mn–120 h old cells. This critical concentration is too low and represents a value $< 1.0\%$ that of Mn+. A critical inhibitory Mn content for the cells of Chlamydomonas reinhardtii has been recorded [12]. A cell requires at least 1.7×10^7 manganese ions in the medium. At lower concentrations (typically <0.5 µM), cells divide more slowly, accumulate less chlorophyll, and the culture reaches stationary phase at lower cell density. *Chlamydomonas* cells do not grow when the manganese supplementation in the medium falls below 0.1 µM [37]. Besides, secondary Fe deficiency results from Mn deficiency and phosphorus is reduced in cells of Chlamydomonas reinhardtii [12].

Manganese deprivation induced also an age-dependent biphasic impact on hydrogenases activity. In the 72 h old cells, both uptake and bidirectional hydrogenases were enhanced in response to Mn deprivation. Older cells of 120 h age exhibited inhibition of Hup but almost unaffected Hox activity by Mn deprivation. However, higher activity of both enzymes was obtained in the older cells (120 h) containing minimal Mn content than in younger cells (72 h). The net activity of both hydrogenases in *Nostoc* seems positive in the sense of hydrogen gas production although nitrogenases might be involved (assays were conducted in buffers devoid of combined nitrogen). Some rates of hydrogen production are comparable with those recorded in *Anabaena* under nitrogen fixing conditions ($BG11_0$) [38]. Magnificent amounts of hydrogen evolution reaching up to 350 µmole $H_2 \cdot mg^{-1}$ $Chl \cdot min^{-1}$ were recorded in 120h Mn double deprived cells

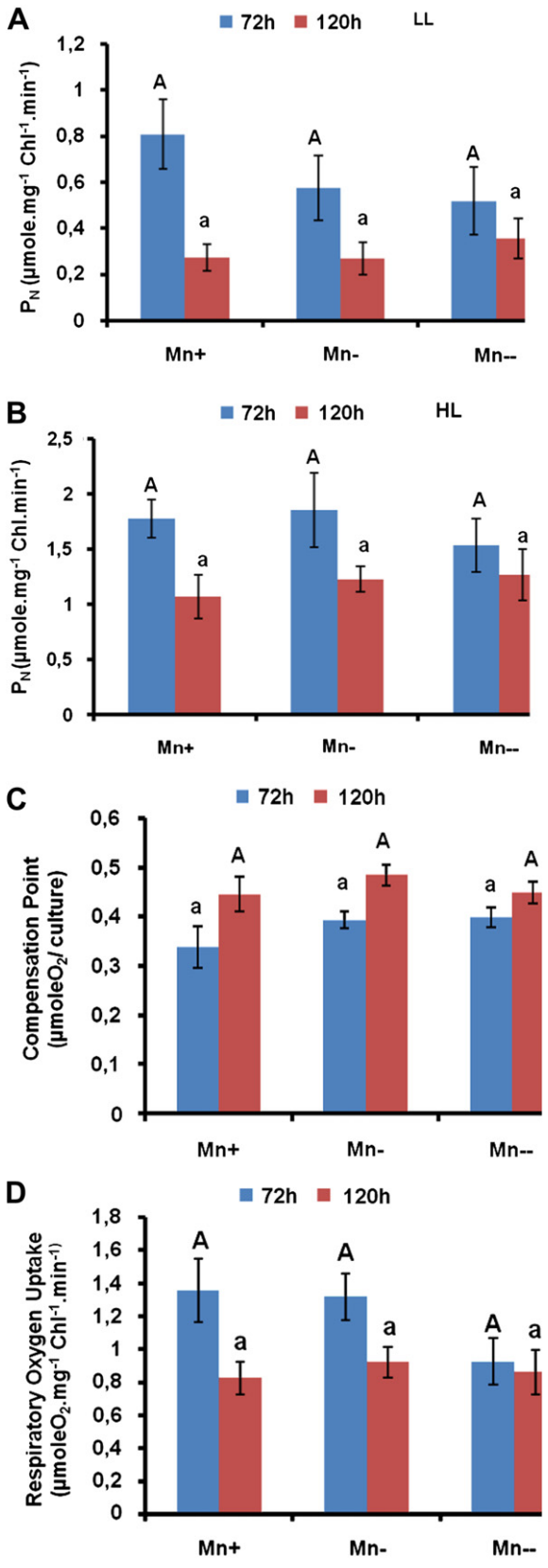

Fig. 6 – (A) Photosynthetic oxygen evolution (P_N) of (Mn+, Mn- and Mn–) *Nostoc*-like strain SAG 2306 cells measured at room temperature under low light intensity of 110 μmole photons.m^{-2}.sec^{-1}. Presented data are means ± SE (n = 8 and 6 for 72 h and 120 h; respectively). Statistical presentations are as in Fig. 3. (B) Photosynthetic oxygen evolution (P_N) of (Mn+, Mn- and Mn–) *Nostoc*-like strain SAG 2306 cells measured at room temperature under high light intensity of 2000 μmole photons.m^{-2}.sec^{-1}. Presented data are means ± SE (n = 8 and 6 for 72 h and 120 h; respectively). Statistical presentations are as in Fig. 3. (C) Oxygen compensation point of (Mn+, Mn- and Mn–) *Nostoc*-like strain SAG 2306 at high light intensity of 2000 μmole photons.m^{-2}.sec^{-1}.It is attained by letting cells photosynthesize a steady state is established. No additives; namely HCO_3^- have been included. Presented data are means ± SE (n = 8 and 6 for 72 h and 120 h; respectively). Statistical presentations are as in Fig. 3. (D) Respiratory oxygen uptake of (Mn+, Mn- and Mn–) *Nostoc*-like strain SAG 2306 in the dark. Presented data are means ± SE (n = 8 and 6 for 72 h and 120 h; respectively). Statistical presentations are as in Fig. 3.

(Mn–) under light and nitrogen fixing (MOPS buffer) conditions. Manganese detoxification by hydrogenases had been very early interlinked. Algae without hydrogenase (*Chlorella vulgaris* and *Chlorella saccharophila*) become rapidly chlorotic under manganese deficiency while chlorophyll is much more stable in those containing hydrogenase (*Chlorella fusca*, *C. vulgaris* f, *Ankistrodesmus braunii* and *Scenedesmus obliquus*) [14]. Also, the cyanobacterium *A. nidulans* developed chlorosis like higher plants under manganese deficiency because it does not have hydrogenase [26]. Since aerobically hydrogenase is inactive, its protective role against manganese deficiency in photosynthesizing algae is questionable. It might be conceivable that like photosynthetic bacteria, cyanobacteria make internal use of hydrogen donors other than molecular hydrogen [14].

Unlike its stimulant effect on biomass accumulation (chlorophyll or dry matter), manganese deprivation inhibited photosynthetic oxygen evolution (P_N) in the *Nostoc*-like strain SAG 2306. Mn(III) and Mn(II) greatly enhanced the photoreduction of 2,6-dichloroindophenol (DCIP) by isolated spinach grana up to a concentration of 80 and 40 μmol dm^{-3}; respectively [39]; Mn was inhibitory at higher concentrations. Below 0.1 μM supplemental Mn the cells are photosynthetically defective due to the accompanying decreased abundance of D1 in C. reinhardtii, which binds the Mn_4Ca cluster [12]. High light intensity (HL) remarkably enhanced P_N of strain SAG 2306 compared with that of low light (LL); but not in a proportional manner with light intensities. The ratio of HL/LL was about 18 times (HL/LL) while photosynthetic rate was enhanced by a factor of only 2.25 times indicating that high light of 2000 μmole photons.m^{-2}.sec^{-1} was over saturating. Only 250 μmole photons·m^{-2} s^{-1} would be enough for light saturated photosynthesis in strain SAG 2306. Over illumination is known to exert negative impacts on photosynthetic apparatus and photosynthesizing cells owing to overreduction by surplus electrons that combine with oxygen (also in excess) leading to formation of peroxide and oxidative stress. Mn-deficient cells of Chlamydomonas reinhardtii are sensitive to peroxide stress due to reduced MnSOD activity [12]. It can be hypothesized that hydrogenases might scavenge electrons (before forming superoxides), reduce protons and form hydrogen molecules.

According to this hypothesis, the role of hydrogenases could be vital to substitute MnSOD in quenching redox effects in Mn deprived cells. This protective effect of hydrogenases as electron scavenger might have led to the observed growth enhancement in Mn deprived strain SAG 2306, supposed to having reduced MnSOD analogous to Mn deprived C. reinhardtii activity [19]. Hydrogenase activation and redox potential are correlated [40]. Once activated the enzyme is not immediately transformed back into an inactive state on rapid reoxidation and is able to preserve its catalytic properties for at least 3–4 h of intense oxygenation [41].

As far as the hydrogenases vulnerability to oxygen is concerned, CO_2 is involved. Cells of cyanobacteria, algae, lichens and higher plants are known to accumulate inorganic carbon via CCM (carbon dioxide concentrating mechanism) when confront limited CO_2 concentrations in their aquatic habitats. CCM is triggered by the CO_2 deprivation signal [42]. Via this CO_2 pump, the total inorganic carbon inside some cyanobacterial cells (e.g. *Anabaena variabilis*) may reach up to 50 mM [43]. In this sense, photosynthesis may continue evolving oxygen and inhibiting hydrogenases without supplementing exogenous carbon source. One approach to avoid photosynthetic oxygen is to deplete cellular reserves of inorganic carbon to attain oxygen compensation point. At this point, interfering oxygen from photosynthesizing carbon reserves to inhibit hydrogenase is ruled out. Oxygen compensation point is assumed to be of significant importance in hydrogen evolution since at this stage O_2 will be readily respired and will not accumulate to inhibitory levels. It seems realistic that maintaining the photosynthesizing cells at the compensation point may save a relevant environment for hydrogenases. In this work, Mn deprivation lowered photosynthesis (P_N), and compensation point (CP) in the 72 h old strain SAG 2306 cells.

In general terms, older cells of 120 h age are characterized by elimination of Mn preferential role in all aspects of photosynthesis (P_N and CP) and furthermore by highest production of hydrogen particularly in the light. At this age, the inhibitory effect of manganese deprivation on photosynthetic characteristics (observed in 72 h old cells) was completely abolished; otherwise a slight increase can be seen in Mn–. This might be explained as the strain SAG 2306 cells attained their critical minimal concentration of Mn that it is no longer a limiting factor. Measuring hydrogen(ases) at the photosynthetic oxygen compensation point will be helpful in future studies of light-dependent hydrogen metabolism that is lacking in many publications. Photosynthetic control of hydrogen metabolism in the cyanobacterium *Oscillatoria chalybea* has been subjected to scrutinized analysis [44,45,46]. The study organism of the present work is under parallel investigations for photosynthesis-hydrogenases interactions [47,48].

5. Conclusion

Aging, *per se*, and manganese deprivation as well as their interaction significantly enhanced hydrogen evolution, particularly in the light. The concentration of 12 μM Mn (in BG11) would be too surplus to suppress growth of *Nostoc* sp SAG 2306 at the early stage (72 h). Mn has its indispensible participation in PSII-catalyzed water oxidation; depletion of which at old, double-deprived cells led to significant inhibition of photosynthetic oxygen evolution that, in turn, enhanced anaerobiosis and subsequently hydrogen evolution.

Acknowledgements

R. A.-B sincerely thanks the Alexander von Humboldt Stiftung for financing his stay in Germany, the group in Botanik III, Universität Düsseldorf for generous hosting, and Stephan Blossfeld for valuable help in assessing photosynthesis. Parts of this work were financed by the German Federal Ministry of Education and Research, BMBF (AlgaTerra project, grant 01 LC 0026) within the BIOLOG program as well as the Deutsche Forschungsgemeinschaft (DFG, FR 905/13-2,3) extended to T.F. T.F. is thankful to Ayoze M. Callicó for his skillful sequencing work, N. Brinkmann for maintenance of the new isolate prior to its accession by the SAG culture collection and I. Kunkel for purification of the strain. N.R. thanks Prof. R. Schulz, Kiel University, for his various supports.

REFERENCES

[1] Azbar N, Dokgöz FTC, Keskin T, Korkmaz KS, Syed HM. Continuous fermentative hydrogen production from cheese whey wastewater under thermophilic anaerobic conditions. Int J Hydrogen Energy 2009;34:7441–7.
[2] Chi Z, Zheng Y, Ma J, Chen S. Oleaginous yeast Cryptococcus curvatus culture with dark fermentation hydrogen production effluent as feedstock for microbial lipid production. Int J Hydrogen Energy 2011;xxx:1–9.
[3] Peixoto G, Saavedra NK, Varesche MBA, Zaiat M. Hydrogen production from soft-drink wastewater in an upflow anaerobic packed-bed reactor. Int J Hydrogen Energy 2011;36:8953–66.
[4] Lea-Langton A, Zin RM, Dupont V, Twigg MV. Biomass pyrolysis oils for hydrogen production using chemical looping reforming. Int J Hydrogen Energy 2011;xxx:1–7.
[5] Kok B, Forbush B, McGloin M. Cooperation of charges in photosynthetic O_2 evolution. I. A linear four step mechanism. Photochem Photobiol 1970;11:467–75.
[6] Joliot P, Kok B. Oxygen evolution in photosynthesis. In: Govindjee, editor. Bioenergetics of photosynthesis. New York: Academic Press; 1975. p. 388–413.
[7] Ke B. Photosynthesis: photobiochemistry and photobiophysics. Dordrecht, The Netherlands: Kluwer; 2001.
[8] Renger G. Photosynthetic water oxidation to molecular oxygen: apparatus and mechanism. Biochim Biophys Acta 2001;1503:210–28.
[9] Kurashov VN, Allakhverdiev SI, Sergey K, Zharmukhamedov SK, Nagata T, Klimov VV, et al. Electrogenic reactions on the donor side of Mn-depleted photosystem II core particles in the presence of $MnCl_2$ and synthetic trinuclear Mn-complexes. Photochem Photobiol Sci 2009;8:162–6.
[10] Zhao W, Guo Q, Zhao J. A membrane-associated Mn-superoxide dismutase protects the photosynthetic apparatus and nitrogenase from oxidative damage in the cyanobacterium *Anabaena* sp. PCC 7120. Plant Cell Physiol 2007;48:563–72.
[11] Wang F-Z, Wang Q-B, Kwon S-Y, Kwak S-S, Su W- A. Enhanced drought tolerance of transgenic rice plants

expressing a pea manganese superoxide dismutase. J Plant Physiol 2005;162:465–72.
[12] Allen MD, Kropat J, Tottey S, Del Campo JA, Merchant SS. Manganese deficiency in *Chlamydomonas* results in loss of photosystem II and MnSOD function, sensitivity to peroxides, and secondary phosphorus and iron deficiency. Plant Physiol 2007;143:263–77.
[13] Yu Q, Rengel Z. Micronutrient deficiency influences plant growth and activities of superoxide dismutases in narrow-leafed lupins. Ann Bot (Lond) 1999;83:175–82.
[14] Kessler E. Effect of manganese deficiency on growth and chlorophyll content of algae with and without hydrogenase. Archiv für Mikrobiologie 1968;63:7–10.
[15] Richter G. Die Auswirkungen von Mangan-Mangel auf Wachstum und Photosynthese bei der Blaualge *Anacystis nidulans*. Planta (berl.) 1961;57:202–14.
[16] Rippka R, Herdman M. Pasteur Culture Collection of cyanobacteria strains in axenic culture. In: Catalogue of strains, Vol. 1. Paris, France: Institut Pasteur; 1992. 103 P.
[17] Hamid A, Morsy FM, Abdel-Basset R. (): Enrichment of heterocysts frequency in a new isolate of *Nostoc* sp SAG 2306 by 2,4-dichlorophenoxyacetic acid and its subsequent impact on modulating photosynthesis/respiration ratio and hydrogenases activities. Egyptian Journal of Phycology (In Press).
[18] Wilmotte A, Van der Auwera G, De Wachter R. Structure of the 16S ribosomal RNA of the thermophilic cyanobacterium *Chlorogloeopsis* HTF ('*Mastigocladus laminosus* HTF') strain PCC7518, and phylogenetic analysis. FEBS Lett 1993;317:96–100.
[19] Siegesmund M, Johansen JR, Karsten U, Friedl T. *Coleofasciculus* gen. nov. (Cyanobacteria): morphological and molecular criteria for revision of the genus *Microcoleus* Gomont. J Phycol 2008;44:1572–85.
[20] Komárek J, Anagnostidis K. Modern approaches to the classification system of Cyanophytes 4-Nostocales. Arch Hydrobiol Suppl 1989;82:247–345.
[21] Castenholz RW. General characteristics of the cyanobacteria. In: Boone DR, Castenholz RW, editors. Bergey's Manual of Systematic Bacteriology. 2nd ed., Vol. 1. New York: Springer; 2001. p. 474–87.
[22] Ludwig W, Strunk O, Westram R, Richter L, Meier H, Yadhukumar A, et al. A software environment for sequence data. Nucleic Acids Res 2004;32:1363–71.
[23] Jobb G. TREEFINDER version of June 2008. Munich, Germany. Distributed by the author at, http://www.treefinder.de; 2008.
[24] Fewer D, Friedl T, Büdel B. *Chroococcidiopsis* and heterocyte-differentiating cyanobacteria are each other's closest living relatives. Mol Phylogenet Evol 2002;23:82–90.
[25] Rodriguez J, Oliver L, Marin A, Medina JR. The general stochastic model of nucleotide substitution. J Theor Biol 1990;142:485–501.
[26] Strimmer K, Rambaut A. Inferring confidence sets of possibly misspecified gene trees. Proc Royal Soc London Ser B 2002;269:137–42.
[27] Kumar S, Tamura K, Nei M. MEGA3: Integrated software for molecular Evolutionary genetics analysis and sequence alignment. Brief Bioinform 2004;5:150–63.
[28] Papaefthimiou D, Hrouzek P, Mugnai MA, Lukesova A, Turicchia S, Rasmussen U, et al. Differential patterns of evolution and distribution of the symbiotic behaviour in nostocacean cyanobacteria. Int J Sys Evol Microbiol 2008;58:553–64.
[29] Anagnostidis K, Komárek J. Modern approaches to the classification system of Cyanophytes 5-Stigonematales. Arch Hydrobiol Suppl 1990;86:1–73.
[30] Gugger MF, Hoffmann L. Polyphyly of true branching cyanobacteria (Stigonematales). Int J Sys Evol Microbiol 2004;54:349–57.
[31] Healy FP. Interacting effects of light and nutrient limitation on the growth rate of *Synechococcus linearis* (Cyanophyceae). J Phycology 1985;21:134–46.
[32] Holden M. Chlorophylls. In: Goodwin TW, editor. Chemistry and biochemistry of plant pigments. 2nd ed., Vol. 2. London: Academic Press; 1976. p. 1–37.
[33] Klimant I, Meyer V, Kühl M. Fiber-Optic oxygen microsensors, a new tool in aquatic biology. Limnol Oceanogr 1995;40:1159–65.
[34] Mus F, Dubini A, Seibert M, Posewitz MC, Grossman AR. Anaerobic acclimation in *Chlamydomonas reinhardtii*, Anoxic gene expression, hydrogenase induction, and metabolic pathways. J Biol Chem 2007;282:25475–86.
[35] Colbeau A, Kelley BC, Vignais PM. Hydrogenase activity in *Rhodopseudomonas capsulata*: relationship with nitrogenase activity. J Bacteriol 1980;144:141–8.
[36] Yu L, Wolin MJ. Hydrogenase measurement with photochemically reduced methyl viologen. J Bacteriol 1969;98:51–5.
[37] Merchant SS, Allen MD, Kropat J, Moseley JL, Long JC, Tottey S, et al. Between a rock and a hard place: trace element nutrition in *Chlamydomonas*. Biochim Biophys Acta 2006;1763:578–94.
[38] Happe T, Schütz K, Böhme H. Transcriptional and mutational analysis of the uptake hydrogenase of the filamentous cyanobacterium *Anabaena variabilis* ATCC 29413. J Bacteriol 2000;182:1624–31.
[39] Amao Y, Ohashi A. Effect of Mn ion on the visible light induced water oxidation activity of photosynthetic organ grana from *spinach*. Catal Commun 2008;10:217–20.
[40] Laurinavichene TV, Zorin NA, Tsygankov AA. Effect of redox potential on activity of hydrogenase 1 and hydrogenase 2 in *Escherichia coli*. Arch Microbiol 2002;178:437–42.
[41] Petrov RR, Utkin IB, Popov VO. Effect of redox potential on the activation of the NAD-dependent hydrogenase from *Alcaigenes eutriophus* Z1. Arch Biochem Buiophys 1989;268:287–97.
[42] Kaplan A, Reinhold L. CO_2 concentrating mechanisms in photosynthetic microorganisms. Annu Rev Plant Physiol Plant Mol Biol 1999;50:539–70.
[43] Ogawa T, Ogren WL. Action spectra for accumulation of inorganic carbon in the cyanobacterium, *Anabaena variabilis*. Photochem Photobiol 1985;41:583–7.
[44]. Abdel-Basset R, Bader KP. Characterization of hydrogen photoevolution in *Oscillatoria chalybea* detected by means of mass spectrometry. Z. Naturforsch 1997;52c:775–81.
[45] Abdel-Basset R, Bader KP. Hydrogen evolution in relation to PSI-reducible substrates in the cyanobacterium *Oscillatoria chalybea* assayed by means of mass spectrometry. Int J Hydrogen Energy 2008;33:2653–9.
[46] Abdel-Basset R, Spiegel S, Bader KP. Saturation of cyanobacterial photoevolution of molecular hydrogen by photosynthetic redox components. J Photochem Photobiology B Biol 1998;47:31–8.
[47] Hamid A, Morsy FM, Abdel-Basset R. Characterization and kinetics of uptake and bidirectional hydrogenase in *Cylindrospermum*. The First International Conference on Biological Sciences (ICBS 2009), Assiut University (Egypt), The Book of Abstracts 2009.
[48] Salah E, Zidan MAA, Abdel-Basset R. Growth and photosynthesis of a cyanobacterium at different concentrations of $MgSO_4$. The First International Conference on Biological Sciences (ICBS 2009), Assiut University (Egypt), The Book of Abstracts 2009.